AD-A142 100 FORCE DISTRIBUTION IN A FRAGMENTED ICE COVER(U) COLD REGIONS RESEARCH AND ENGINEERING LAB HANOVER NH D STEWART ET AL. MAR 84 CRREL-84-7 1/1

UNCLASSIFIED F/G 8/12 NL

END
DATE
FILMED
7-84
DTIC

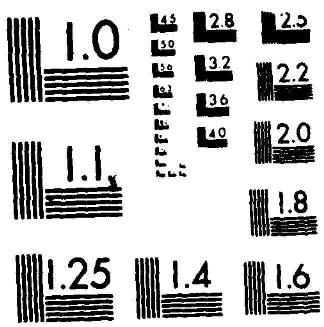

MICROCOPY RESOLUTION TEST CHART
NATIONAL BUREAU OF STANDARDS 1963 A

CRREL REPORT 84-7

US Army Corps of Engineers
Cold Regions Research & Engineering Laboratory

Force distribution in a fragmented ice cover

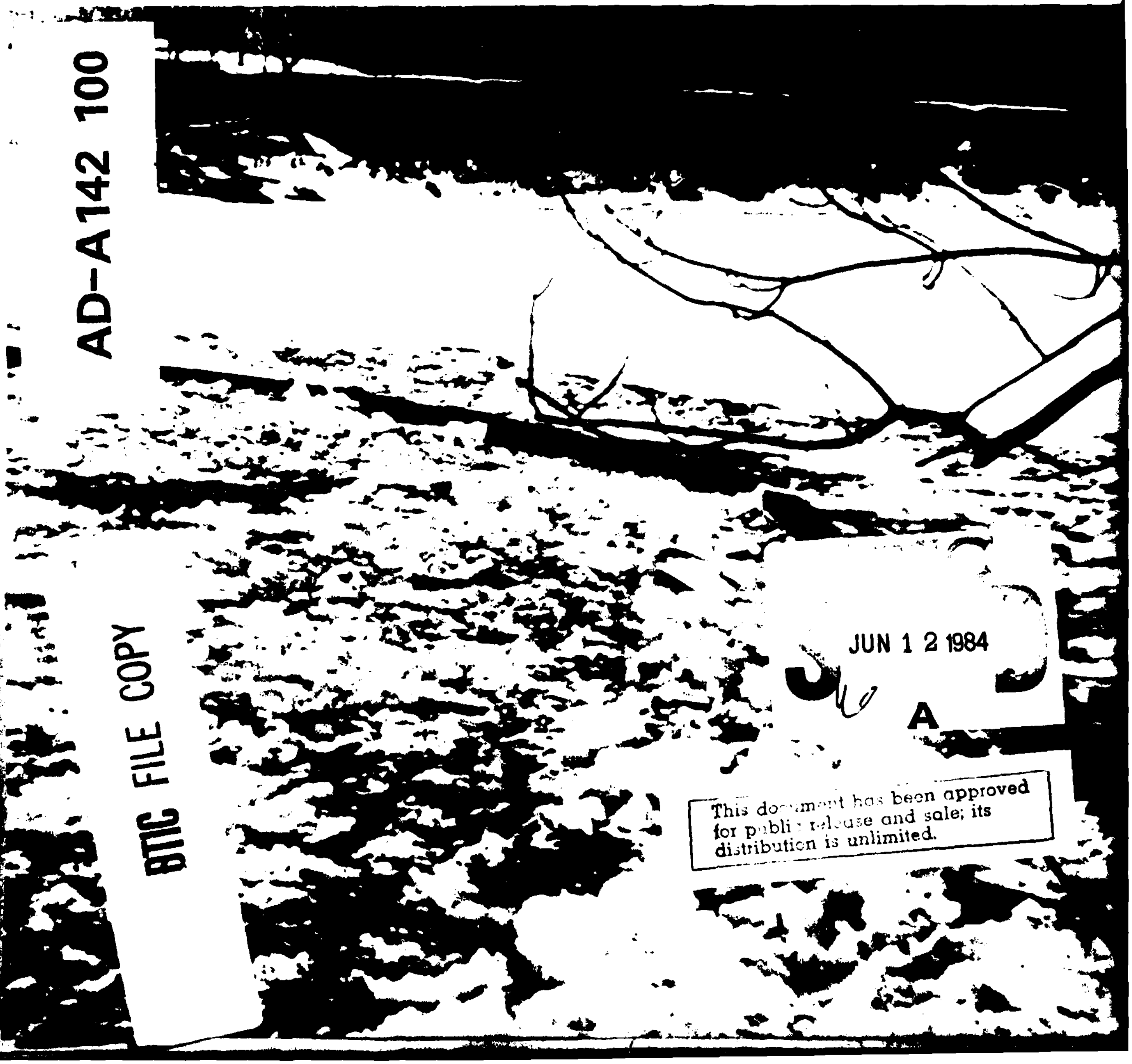

For conversion of SI metric units to U.S./British customary units of measurements consult ASTM Standard E380, Metric Practice Guide, *published by the American Society for Testing and Materials, 1916 Race St., Philadelphia, Pa. 19103.*

Cover: Fragmented ice cover restrained by an ice boom.

Unclassified

SECURITY CLASSIFICATION OF THIS PAGE (When Data Entered)

REPORT DOCUMENTATION PAGE		READ INSTRUCTIONS BEFORE COMPLETING FORM
1. REPORT NUMBER CRREL Report 84-7	2. GOVT ACCESSION NO. AD-A142100	3. RECIPIENT'S CATALOG NUMBER
4. TITLE (and Subtitle) FORCE DISTRIBUTION IN A FRAGMENTED ICE COVER		5. TYPE OF REPORT & PERIOD COVERED
		6. PERFORMING ORG. REPORT NUMBER
7. AUTHOR(s) Douglas Stewart and Steven F. Daly		8. CONTRACT OR GRANT NUMBER(s)
9. PERFORMING ORGANIZATION NAME AND ADDRESS U.S. Army Cold Regions Research and Engineering Laboratory Hanover, New Hampshire 03755		10. PROGRAM ELEMENT, PROJECT, TASK AREA & WORK UNIT NUMBERS DA Project 4A161101A91D
11. CONTROLLING OFFICE NAME AND ADDRESS		12. REPORT DATE March 1984
		13. NUMBER OF PAGES 22
14. MONITORING AGENCY NAME & ADDRESS(If different from Controlling Office)		15. SECURITY CLASS. (of this report) Unclassified
		15a. DECLASSIFICATION/DOWNGRADING SCHEDULE

16. DISTRIBUTION STATEMENT (of this Report)

Approved for public release; distribution unlimited.

17. DISTRIBUTION STATEMENT (of the abstract entered in Block 20, if different from Report)

18. SUPPLEMENTARY NOTES

19. KEY WORDS (Continue on reverse side if necessary and identify by block number)

Flume tests
Ice
Ice booms
Ice forces
Laboratory tests
River ice

20. ABSTRACT (Continue on reverse side if necessary and identify by block number)

Experiments were conducted in CRREL's refrigerated flume facility to examine the two-dimensional force distribution of a floating, fragmented ice cover restrained by a boom in a simulated river channel. To determine the force distribution, a vertically walled channel, instrumented for measuring normal and tangential forces, and an instrumented restraining boom were installed in a 40.0- by 1.3-m flume. Two sizes of polyethylene blocks and two similar sizes of freshwater ice blocks were tested using water velocities ranging from 10 to 30 cm/s. The forces measured at the instrumented boom leveled off with increasing cover length. The contribution of the increasing shear forces developed along the shorelines to this leveling off in the data was clearly evident. The shear coefficients of the polyethylene blocks averaged 0.43, and the freshwater ice averaged 0.044. The normal force measured along the instrumented shoreline could not be

DD FORM 1 JAN 73 1473 EDITION OF 1 NOV 65 IS OBSOLETE

Unclassified

SECURITY CLASSIFICATION OF THIS PAGE (When Data Entered)

20. Abstract (cont'd).

related simply by a K coefficient to the longitudinal force; another expression was required, with a term being a function of the cover thickness and independent of the undercover shear stress or cover length. By adding this term, good agreement was then found between the measured and predicted values of the boom forces and the shoreline normal and shear forces.

CRREL Report 84-7

March 1984

Force distribution in a fragmented ice cover

Douglas Stewart and Steven F. Daly

PREFACE

This report was prepared by Douglas Stewart, former Civil Engineer, and Steven F. Daly, Research Hydraulic Engineer, of the Ice Engineering Research Branch, Experimental Engineering Division, U.S. Army Cold Regions Research and Engineering Laboratory. Funding for this research was provided by In-House Laboratory Independent Research, DA Project 4A161101A91D.

The authors express their appreciation to Dr. Devinder Sodhi and F. Donald Haynes for technical review of this report. The authors also express their gratitude to Dr. Sodhi for his many helpful suggestions and for the insight he provided.

The contents of this report are not to be used for advertising or promotional purposes. Citation of brand names does not constitute an official endorsement or approval of the use of such commercial products.

CONTENTS

ILLUSTRATIONS

TABLES

FORCE DISTRIBUTION IN A FRAGMENTED ICE COVER

Douglas Stewart and Steven F. Daly

A-1

INTRODUCTION

It has only been in recent years that the systematic study of the mechanics and hydraulics of fragmented river ice covers has been undertaken. The complex, random and often fearsome nature of the many phenomena that constitute ice processes seems to defy any analytical approach to the problem. However, the growing interaction between man and ice, as shown by the development of ice booms and other ice control structures, and the need for winter navigation on ice-covered waters demand some rational basis for design and planning. As an initial step, the ability to predict forces produced by a fragmented ice cover on a shoreline and on downstream restraints is essential. Theories have been developed that describe the force distribution in fragemented ice covers, largely through analogies with other fields of study, principally soil mechanics and the mechanics of hopper and bin design. However, experimental or field data are scarce and these theories remain, by and large, untested.

In this study, we investigated the force distribution in a floating, fragmented ice cover restrained by a boom in a simulated channel. To determine the force distribution, force measurement panels, instrumented for measuring normal and shear forces, and an instrumented restraining boom were installed in a refrigerated flume. Two sizes of polyethylene blocks and two similar sizes of freshwater ice blocks made up the ice covers. Tests were conducted with water velocities ranging from 10 to 30 cm/s. The total load on the boom as a function of cover length and water velocity was measured, as were the normal and shear forces along the shoreline.

EXPERIMENTS

Test flume facility

CRREL's flume is 40.0 m long, 1.3 m wide and 0.6 m deep. It has a slope range of −0.0009 to 0.018, and is tilted by an automatic coordinated jacking system. The flow capacity is variable from 0 to 0.4 m^3/s and is monitored by in-line magnetic flowmeters. The water level in the flume can be controlled with either a submersible head gate, a tail gate or a series of adjustable vertical louver gates located in the tailbox. The flume is located in a room that can be cooled to -29°C by a liquid ammonia refrigeration system. A refrigerated coil in the water storage tank can chill the test water before it enters the flume.

Experimental apparatus

The experimental apparatus consisted of an instrumented restraining boom and 10 force measurement panels installed upstream of the boom along the walls of the flume. The boom was constructed of wood and wire screen. The forces transmitted to it were measured by two aluminum rods instrumented with strain gauges. These rods were instrumented in the same way as the support rods of the force measurement panels, described below.

There were 10 separate 91-cm by 15.2-cm polyethylene force measurement panels suspended

Table 1. Test series.

Exp. No.	Date (day/mo.)	Flume discharge Gal/min.	Flume discharge m^3/s ($\times10^{-2}$)	Water velocity (cm/s) Calculated U*	Water velocity (cm/s) Calculated D†	Water velocity (cm/s) Under jam	Water velocity (cm/s) Measured U	Water velocity (cm/s) Measured D	Froude $v/\sqrt{gh}$ D	Froude Under Jam	Flow depth (cm)	Room temp. (°C)	Water temp. (°C)	Avg. jam thickness (cm)	Jam length (m)	Thickness of ice blocks (mm) Before Mean	Before S.D.	After Mean	After S.D.
									4-in. plastic blocks										
42**	27/12	500	3.2	11.09	11.72	14.90	-	-	0.017	0.101	27.94	12.8	-	6.04	7.31	-	-	-	-
43**	28/12	500	3.2	11.70	12.30	14.90	-	-	0.076	0.101	26.67	12.8	-	4.63	7.31	-	-	-	-
44**	28/12	750	4.7	17.20	18.10	21.90	-	-	0.112	0.150	26.67	12.8	-	4.63	7.31	-	-	-	-
46**	3/1	400	2.5	8.67	9.15	11.70	-	-	0.055	0.080	27.94	12.8	-	6.04	7.31	-	-	-	-
48	4/1	600	3.8	12.90	13.70	17.70	12.0	10.0	0.082	0.120	28.26	12.8	4.40	6.40	7.31	-	-	-	-
49	7/1	750	4.7	16.30	17.20	21.90	14.0	12.0	0.104	0.150	27.94	12.8	0.61	6.04	7.31	-	-	-	-
50	8/1	600	3.8	12.50	13.30	19.90	10.0	10.0	0.079	0.144	29.20	12.8	6.10	10.20	6.40	-	-	-	-
									2-in. plastic blocks										
54	21/1	750	4.7	15.40	16.40	23.30	18.0	-	0.097	0.163	29.27	12.8	1.67	8.89	8.23	-	-	-	-
55	21/1	750	4.7	15.70	16.70	30.90	10.0	-	0.099	0.250	28.80	12.8	3.90	14.10	5.49	-	-	-	-
56	22/1	600	3.8	12.70	13.40	21.40	11.0	13.0	0.079	0.160	28.90	12.8	3.90	11.30	7.31	-	-	-	-
57	22/1	600	3.8	12.70	13.40	16.20	12.5	10.5	0.079	0.105	28.90	12.8	3.90	4.75	9.14	-	-	-	-
58	22/1	500	3.2	10.10	10.80	14.70	10.5	9.5	0.063	0.099	30.22	12.8	3.90	8.13	6.40	-	-	-	-
59	22/1	500	3.2	10.30	10.90	12.99	10.0	12.0	0.064	0.082	29.80	12.8	3.90	4.32	9.14	-	-	-	-
60	22/1	400	2.5	8.97	9.45	12.90	6.0	6.0	0.058	0.092	27.13	12.8	4.40	7.50	9.14	-	-	-	-
									4-in. ice blocks										
63	25/1	400	2.5	9.13	9.60	10.80	8.0	8.0	0.059	0.071	26.73	4.4	0.00	2.67	5.48	-	-	-	-
64††	28/1	400	2.5	8.79	9.28	9.92	9.0	8.5	0.056	0.062	27.59	4.4	1.10	2.50	5.48	7.10	1.60	4.50	1.20
65	29/1	500	3.2	10.39	11.02	12.75	-	10.5	0.065	0.080	29.55	-0.3	0.00	3.50	5.48	11.85	3.60	11.80	2.60
66	30/1	600	3.8	12.96	13.70	16.50	-	12.5	0.082	0.108	28.33	-1.7	0.83	4.69	5.48	11.44	2.90	11.80	2.40
67	31/1	700	4.4	14.50	15.40	22.50	-	14.5	0.091	0.160	29.18	0.5	0.40	9.53	5.48	13.64	2.70	14.29	2.70
68	1/2	750	4.7	16.90	17.80	26.80	-	20.0	0.109	0.205	27.03	1.7	0.28	10.16	6.40	16.09	2.40	15.13	3.90
69	2/2	750	4.7	16.80	17.70	31.80	-	18.0	0.108	0.261	27.20	1.6	0.30	12.83	4.57	17.06	2.70	16.70	2.90
									2-in. ice blocks										
70	6/2	400	2.5	8.80	9.30	11.30	-	8.0	0.057	0.076	27.51	1.7	0.50	4.67	8.23	18.21	4.67	16.13	6.80
72	7/2	500	3.2	11.70	12.28	14.52	-	9.0	0.076	0.097	26.75	2.2	1.10	3.94	5.48	14.10	5.86	11.60	3.90
73	8/2	600	3.8	13.50	14.20	19.30	10.0	12.0	0.087	0.137	27.45	1.1	0.40	7.49	7.32	16.11	6.62	15.70	3.97
74	9/2	700	4.4	15.70	16.60	23.60	23.0	23.0	0.102	0.172	27.30	1.7	0.30	8.38	5.48	17.02	5.17	12.93	3.79
75	12/2	750	4.7	16.04	16.90	24.30	18.0	18.0	0.101	0.161	28.30	4.4	0.40	7.62	5.79	12.30	4.04	10.20	4.74

* Measured immediately upstream of ice jam.
† Measured immediately downstream of ice jam.
** For these experiments jam thickness data were not available. Thicknesses were estimated for the calculations.
†† Extensive melting of ice blocks occurred during this test.

parallel to the flume walls by 1.9-cm-diameter aluminum support rods instrumented with strain gauges. Five measurement panels were suspended on each side of the flume. Each pair of opposing panels defined a test section–there were five tests sections in total. Each panel was bolted vertically through its center point to the support rod, and the support rods were bolted to a rigid overhead frame that was secured to the flume body. Each support rod had a milled section located 30 cm above the panel. The milled sections had four flat vertical faces, upon which two pairs of linear displacement strain gauges were mounted. Movement of the panel in the horizontal plane was transmitted to the gauges through the bending of the rod. The rods were mounted in the support frame so that one pair of strain gauges was oriented in the direction of water flow and the other pair transverse to the flow. In this configuration, the pair of gauges oriented with the flow direction indicated the shear force, and the transversely mounted pair indicated the normal force. Figure 1 shows the details of the force measurement panels and the supporting frame. After calibration of the support rods and panels, an unknown load could be measured by observing the readings from the strain gauges on each rod.

Each pair of strain gauges was wired into a data logger as a two-active-arm wheatstone bridge. The data logger was used to complete the wheatstone bridge and to provide analog-to-digital processing for interfacing with an HP9845 digital computer. The HP9845 computer served as the controller for the data logger, stored data on flexible discs, and performed some real time processing.

Experimental procedure

The test series is outlined in Table 1. The ice covers ranged from 6 to 150 mm thick and were relatively uniform along their lengths. These values are also presented in Table 1. The ice cover thicknesses were measured by inserting a vertical rule through the cover along the centerline of the flume. These thickness measurements were taken at the midpoint of each panel section.

The plastic blocks were cut from commercially available polyethylene sheets with a band saw; their dimensions were 51 by 51 by 6.5 mm (2 by 2 by ¼ in.) and 102 by 102 by 6.5 mm (4 by 4 by ¼ in.). The polyethylene had a specific gravity of 0.92, very close to the specific gravity of freshwater ice.

The freshwater ice blocks were frozen in trays near the headbox of the flume and placed in the flume at that point. The dimensions of the ice blocks were also 51 by 51 mm and 102 by 102 mm. The thickness of the individual ice blocks varied slightly but on the average were the same as the plastic blocks. The thickness values are presented in Table 1.

A typical test proceeded as follows: The water discharge through the flume was set and the proper water elevation through the test section obtained. The initial forces on the force measurement panels caused by the water flow were measured without the boom in place. The boom was then attached to its two support rods and forces were measured again.

The model ice floes, made of either the polyethylene or freshwater ice, were then placed in the flume upstream of the instrumented sections and allowed to float into position behind the instrumented boom. The floating cover was manually stirred to increase the randomness of the individual ice floes because they would often align themselves in a very regular manner in the ice cover. Also, for the experiments at the lower discharge rates, the water velocity was not sufficient to underturn the floes. An ice cover only one floe thick would not transmit enough force to be measured. Stirring then had the additional effect of thickening the cover. Rakes, or dividers, were placed into the ice cover between the force measurement panels and the ice cover was broken up into segments, with the length of a segment equal to the length of a force measurement panel. To assure that the velocity profile was fully developed, a floating sheet of polyethylene was placed immediately upstream of the ice cover to act as an extension of the cover. This polyethylene sheet was restrained so that it did not touch the fragmented cover and contribute to the force within it.

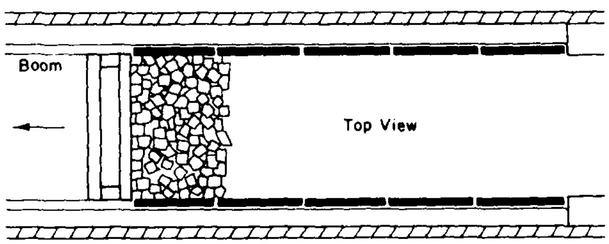

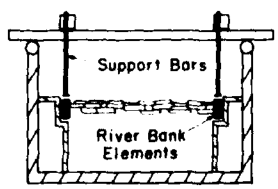

Figure 1. Details of force measurement panels and supporting frame.

The force transmitted to the boom and the shear and normal forces transmitted to the measurement panels were measured simultaneously. Three measurements of the force levels were taken for each cover length investigated. Each force measurement was the average of 32 readings that were taken within approximately 2 seconds. After the three measurements were taken, a rake was removed and the cover length incrementally increased. The measurements were then repeated and the cover length incrementally increased again. Each incremental increase in cover length was approximately equal to the width of the flume. Typically, the maximum ice cover length was greater than the instrumented section. At this length the boom force resulting from the total length of the jam could be measured but the shoreline forces could only be measured in the instrumented section (the instrumented section extended for five ice cover widths upstream from the boom).

After all the rakes had been removed from the jam and the force readings completed, the boom was removed and the model floes were released from the measurement section. For each test sequence, the water level, flow velocity, cover thickness along the flume's centerline, ambient air temperature, water temperature, and cover length were measured and recorded. When the ice blocks were used, the thickness of the blocks at the start and end of the experiment were measured to see how much they had melted. These data are presented in Table 1.

RESULTS

Plastic versus freshwater ice

At the onset of this investigation the extent to which the distribution of forces would differ between the freshwater ice blocks and the polyethylene blocks was not known. Tatinclaux et al. (1977) discussed the effect of water surface tension on ice modeling materials, but their concern was modeling the incipient submergence velocity of model ice floes. The effect of the surface tension interaction of the two materials with the polyethylene force measurement panels was significant. The shear forces measured by the force measurement panels differed considerably between the polyethylene blocks and the freshwater ice blocks.

We believe that the polyethylene blocks tended to develop greater shear with the force measurement panels because of an adhesive force from surface tension. On the other hand, the freshwater ice blocks had a small water layer between them and the force measurement panels. On the smooth surface of the force measurement panels, this slight water layer significantly changed the coefficient of friction between the freshwater ice blocks and the force measurement panels. Force measurement panels with greater surface roughness may minimize this difference in measured shear forces. In addition, melting of the freshwater ice blocks would influence the force that the freshwater cover would be able to transmit. This would also tend to reduce the measured shear forces.

Shoreline forces

The reactions measured along the shorelines by the force measurement panels were of two types: shear forces, parallel to the directi^n of the water

Table 2. Average parameters f ach experiment. Coefficient of friction, coefficien proportionality, f_{no} (see p. 9) and β (see p. 7) determi h experiment. These parameters were determined ing the best fit linear relationship between two sets of data.

Exper. No.	Coef. of friction (μ)	Coef. of proportionality (K)	f_{no}	β
		4-in. plastic blocks		
42	0.329	0.249	55.46	0.093
43	0.134	0.341	36.99	0.038
44	0.423	0.146	30.23	0.036
46	-0.043	-0.168	48.34	0.180
48	0.539	0.211	65.15	0.055
49	0.652	0.164	42.15	0.121
50	0.453	0.096	26.12	0.042
Avg.	0.471	0.134	–	0.067
		2-in. plastic blocks		
54	0.762	0.455	36.00	0.193
55	0.369	0.621	119.27	0.359
56	0.635	0.339	72.92	0.105
57	0.405	0.479	9.65	0.174
58	0.673	0.175	38.62	0.075
59	0.334	0.332	5.22	0.105
60	0.125	0.288	35.69	-0.025
Avg.	0.399	0.384	–	–
		4-in. ice blocks		
63	0.651	0.174	3.34	0.162
64	0.096	-0.078	6.88	0.048
65	-0.037	-0.206	16.56	0.089
66	-0.025	0.155	20.03	0.009
67	0.087	0.086	83.61	0.011
68	0.220	-0.022	117.08	-0.076
69	0.043	0.056	197.26	0.001
Avg.	0.027	0.203	–	0.038
		2-in. ice blocks		
70	0.076	0.002	19.69	0.088
72	0.008	-0.009	56.98	0.004
73	0.025	0.065	155.42	0.023
74	0.197	0.201	86.65	0.033
75	-0.014	0.248	155.36	0.016
Avg.	0.063	0.252	–	0.037

flow, and normal forces, perpendicular to the direction of the water flow. The shear and normal forces measured by the opposing force measurement panels in a section were averaged to provide the average shear force and the average normal force for that section. The average shear forces and the average normal forces measured in each test section were correlated and this correlation was the coefficient of friction between the ice modeling material and the force measurement panels. The average measured coefficient of friction was 0.044 for the freshwater blocks and 0.43 for the polyethylene blocks. The results for each test are shown in Table 2. This difference in coefficients is probably a result of the factors noted earlier. The average shear force and average normal force measured in each section are listed in Appendix A.

Boom forces

The boom force data are plotted in Figure 2. The measured values are listed in Appendix A. From the figure it can be seen that, in general, as the ice cover length was increased, a length was reached beyond which no additional forces were transmitted to the boom. For the ice covers formed by polyethylene blocks, the force felt by the boom reached its peak when the cover was about four to five river widths in length. For ice covers formed by freshwater ice blocks, the force felt by the boom reached its peak when the ice cover was substantially longer.

The different lengths at which the boom forces reached a maximum are probably strongly influenced by the different coefficients of friction between the modeling materials and the force measurement panels. The larger coefficient of friction developed by the polyethylene blocks allowed a proportionately larger share of the shear force produced by the water flowing under the cover to be resisted by a given length of shoreline. Thus as the ice cover grew in length, a length was reached at which all the additional force created by an increase in the cover length was resisted by the shoreline. This length was a function of the coefficient of friction between the ice cover and the shoreline. This finding is in general agreement with the findings of earlier investigators and will be discussed further in the *Discussion*. The leveling off of the boom forces strongly parallels that of the measured vertical forces at the bottom of grain bins and silos, which also reach a maximum at some depth. Beyond this depth all the gravitational force on the grain is transferred to the bin walls by friction.

Average shear stress under the ice cover

To determine the average shear stress under the ice cover, the downstream components of the forces on the restraining boom and the force measurement panels were summed and divided by the total area of the cover being measured. The shear stresses are tabulated in Appendix A.

Internal forces

The average force in the downstream, longitudinal direction within the cover was calculated by a free body force analysis using simple statics. The average downstream, longitudinal force within the cover was calculated at the upstream end of each measurement panel by the formula

$$f_{us} = f_{ds} + f_s - \tau A \qquad (1)$$

where f_{us} = average internal force at upstream end of a measurement section

f_{ds} = average internal force at the downstream end of a measurement section

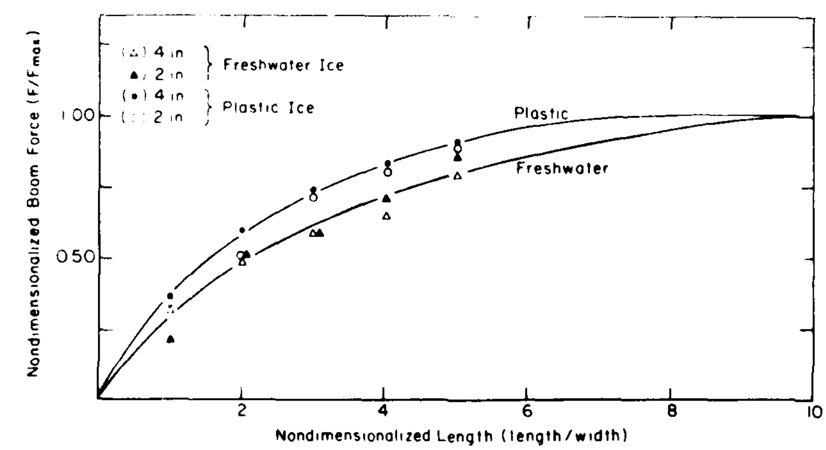

Figure 2. Boom force data.

f_s = shear force measured by the force measurement panels
τ = calculated shear produced by flowing water
A = area of the cover.

The force at the downstream point was always known; this was the force felt by the restraining boom. The force at the upstream end of the cover was always zero owing to the presence of the rakes. The average internal force in the downstream direction in the ice cover could then be calculated between each pair of opposing force measurement panels. The internal force was assumed to vary linearly between the upstream end and downstream end of each force measurement panel; therefore, the average internal forces were determined to be the average of f_{us} and f_{ds}. For those experiments where the ice cover extended beyond the length of the measurement section of the flume, the total force in the downstream direction was not known. Consequently, the average undercover shear or the internal forces within the cover could not be calculated.

DISCUSSION

The forces that can act on a fragmented ice cover include the hydrodynamic force of current against the upstream limit of the cover, the shearing stress of the water flowing under the cover, the weight of the cover and pore water in the direction of the slope of the water surface, the shearing stress of the wind over the cover, the reaction of the banks and the reaction of any downstream restraint. In this experiment many of these forces were greatly eliminated. A polyethylene sheet placed immediately upstream of the fragmented cover eliminated

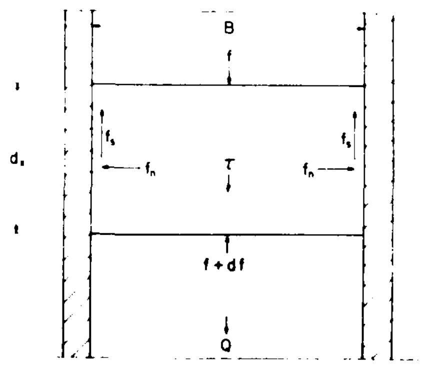

Figure 3. Force balance on a two-dimensional elemental length of the fragmented cover.

the hydrodynamic force against the upstream limit of the cover. The water surface was nearly horizontal as the flume is very smooth (polished aluminum). As a result, the component of the weight of the cover in the downstream direction was essentially zero. There was no wind stress. The reaction of the banks and the reaction of the restraining boom were carefully measured. So, the only force on the fragmented cover was the shear stress of the water flowing under it.

A force balance on a two-dimensional elemental length of the fragmented cover is shown in Figure 3. If any cohesion between the shore and the ice cover is ignored, this force balance can be expressed as

$$Bf + \tau B dx = 2 f_s dx + (f + df)B \tag{2}$$

or, in differential form, as

$$\frac{df}{dx} + \frac{2f_s}{B} = \tau \tag{3}$$

where τ = shear stress exerted on the bottom of the cover by the flowing water
f = average force per unit width from the longitudinal stress
f_s = shear force reaction per unit length along the channel
B = width of the channel
f_n = average force normal to the banks per unit length.

This is an expression of the static equilibrium among the forces acting on a two-dimensional elemental length and extending over the full width and thickness of the cover.

To facilitate integration of eq 3, several assumptions must be made. The first is that the relation between shear and normal forces along the shoreline can be expressed as

$$f_s = \mu f_n \tag{4}$$

where μ is the coefficient of friction. The calculated coefficients of friction are listed in Table 2. As has been previously noted, a significant difference was found between the coefficients of friction for the plastic and freshwater ice.

The second assumption is that the relation between the average force in the downstream, longitudinal direction in the ice cover and the average normal force measured at the shoreline can be expressed as

$$f_n = Kf. \tag{5}$$

K can be considered a coefficient of proportionality between the longitudinal and normal forces. The calculated values of K are listed in Table 2. Finally, by substitution

$$f_s = \mu K f. \tag{6}$$

The validity of the assumptions that led to eq 6 can be examined with the data obtained in this experiment. From the measured shear and normal forces the coefficient of friction can be determined. The calculated coefficients of friction are shown in Table 2. Next, the coefficient of proportionality K can be determined by correlating the average normal force and the average internal force in the downstream longitudinal direction in each section. The calculated coefficients for each test are shown in Table 2. Similarly, the correlation between the average measured shear force and the average internal force in the downstream, longitudinal direction in each section can be determined for each test. For clarity this coefficient will be referred to as β; β should be equal to the product of coefficient of friction (μ) and the coefficient of proportionality (K). That is

$$f_s = \beta f. \tag{7}$$

The values of β for each test are shown in Table 2, and the values of β and the product μK are compared in Figure 4. It can be seen that the comparison is, in general, good. The freshwater ice shows considerably more scatter than the polyethylene ice. Factors causing this scatter will be examined later.

Now, substituting eq 6 into eq 3 we arrive at

$$\frac{df}{dx} = \frac{2\mu K f}{B} - \tau = 0. \tag{8}$$

Integrating and setting $f = 0$ at the boundary condition $x = 0$

$$f = \frac{\tau B}{2\mu K}\left(1 - e^{\frac{-2\mu K x}{B}}\right). \tag{9}$$

This is the expression for the longitudinal force transmitted by a fragmented cover. This equation is essentially similar to those derived by Pariset and Hausser (1961), Berdennikov (1964), Sodhi and Weeks (1978) and Michel (1978). The equation predicts that a boom will experience a maximum force equal to $\tau B/2\mu K$ and that this force level will be approached asymptotically as the ice cover length x is increased. The boom forces measured in this experiment followed this pattern. The dependence of the maximum force experienced by the boom on the coefficient of friction μ between the ice cover and shoreline, as has been noted, can also be seen.

The product μK can also be determined by a nonlinear regression analysis of eq 9 using the measured boom force f, cover length x, channel width B, and the calculated undercover shear stress τ. A comparison of the μK values determined by nonlinear regression and the β values listed in Table 2 is shown in Figure 5. It can be seen that the parameters derived from eq 9 are approximately twice those of the values listed in Table 2.

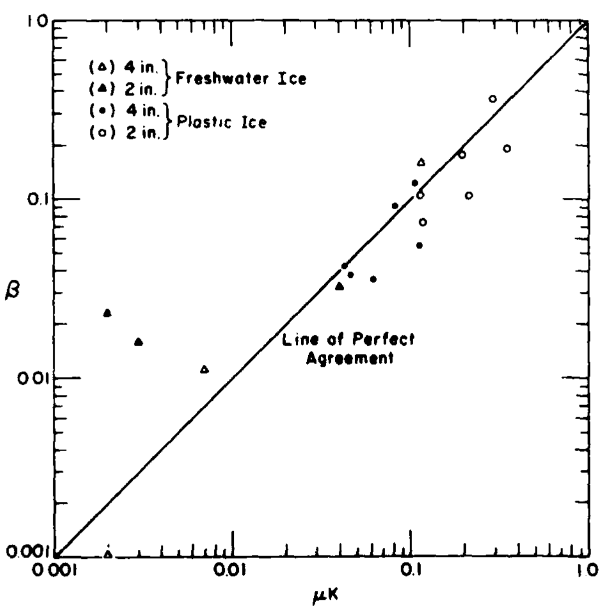

Figure 4. Comparison of the product of μ and K to the value of β derived from eq 7.

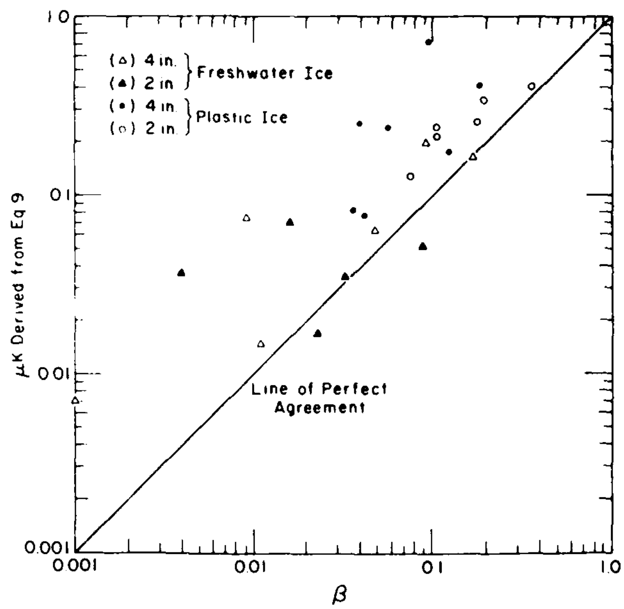

Figure 5. Comparison of the value of μK derived from eq 9 and the value of β derived from eq 7.

What are the possible reasons for the discrepancies between the two sets of values for the product of μ and K? The coefficient of friction μ is a straightforward ratio of two measured forces. However, K, the coefficient of proportionality, is somewhat more ambiguous. The basis of the above set of equations starts with Janssen's (1895) theory of silo loading. Janssen assumed that the horizontal pressure in a silo or bin was a constant ratio, K, to the vertical pressure. He indicated that the value of K was to be determined experimentally, and values for K have been determined for many materials that are stored in silos and bins. Typical values range from 0.38 to 0.61. Analogously, Pariset et al. (1966) defined this parameter as the relation between the longitudinal stress and the "transversal stress pushing the [ice] cover against the bank." This definition leads immediately to eq 5, except that in eq 5 the average longitudinal force and average normal force on the shoreline are equated. (As the area of the force measurement panels and the cross-sectional area of the cover were virtually identical, forces and stresses can be used interchangeably in this analysis.) Cowin (1977) has shown that Janssen's K coefficient should be interpreted "as the ratio of the horizontal stress averaged over the lateral boundary perimeter to the vertical stress averaged over the cross sectional area of the bin." Sodhi and Weeks (1978) used this interpretation in their derivation of the force balance in a fragmented cover, and we have followed their example.

It can be seen then that the coefficient of proportionality, K, is a concept that we borrowed from bin and silo loading and applied to fragmented ice covers. However, there are several conditions that exist in fragmented ice covers that are very different from those in bins and silos. The first and most obvious is the presence of free surfaces. Essentially, two free surfaces exist for fragmented ice covers. One allows displacement upwards, which is resisted by gravity; the second allows displacement downwards, which is resisted by the buoyancy force of the ice. A second major difference is that two major body forces act on the ice field, rather than the single body force of gravity in the silo. In the analysis of the forces in an ice cover, the shear force of the flowing water was assumed to be analogous to the gravity force in the silo loading theory. There is no analogous force in silo theory to the buoyancy and gravity forces experienced by the ice cover. As noted by Mellor (1979), if the thickness of a cohesionless ice cover is greater than the typical fragment size, then the ice cover must be confined. An unconfined cover would spread out until it was one fragment thick. Therefore, even if no shear force is applied by the flowing water, the shoreline will experience a normal force because it keeps the fragmented cover from spreading. This normal force required to restrain the cover within the shoreline will be a component of the average normal forces that were measured. This component should appear as the value of f_n when the average longitudinal force,

f, is set to zero. This component then should be the intercept of the relationship

$$f_n = Kf + f_{no} \tag{10}$$

determined from the measured forces. In Figure 6, this intercept f_{no} is plotted as a function of the average cover thickness–a relationship can be readily seen. Equation 6 can now be modified to

$$f_s = \mu Kf + \mu f_{no} \, . \tag{11}$$

Equation 8 therefore becomes

$$\frac{df}{dx} + \frac{2\mu Kf}{B} + \frac{2\mu f_{no}}{B} - \tau = 0 \tag{12}$$

and eq 9 becomes

$$f = (\frac{\tau B}{2\mu K} - \frac{f_{no}}{K})(1 - e^{\frac{-2\mu Kx}{B}}) \, . \tag{13}$$

At first this formula seems artificial. If the undercover shear stress τ is reduced to zero, can a negative longitudinal force transmitted through the cover be possible? If τ was reduced to zero, the cover would be unrestrained in the longitudinal direction. The cover would then attempt to spread out by moving upstream. This *would* produce a negative force in the longitudinal direction.

Using the values of f_{no} and K from Table 2, we can derive the value of product μK by nonlinear regression of eq 13. The comparison of these values with β in Table 2 is shown in Figure 7. A much better fit of μK from eq 12 to β from Table 2 can be noted, although considerable scatter exists, especially for the freshwater ice.

It is interesting to note that a good fit can be achieved using the measured boom force and the ice cover thickness averaged over the entire cover. If we substitute eq 10 into eq 13, an expression for the distribution of the normal forces can be derived:

$$f_n = (\frac{\tau B}{2\mu} - f_{no})(1 - e^{\frac{-2\mu Kx}{B}}) + f_{no} \, . \tag{14}$$

Values of μK and of μ can be determined using nonlinear regression. However, there is tremendous scatter when these values are compared to the values in Table 2. The forces experienced by a boom are a function of the *average* values of the parameters of the upstream cover. The normal forces experienced by the shoreline, however, reflect the local conditions of the ice cover opposite the shoreline at that point. Therefore, predicting the normal forces is a much more difficult matter than predicting the forces

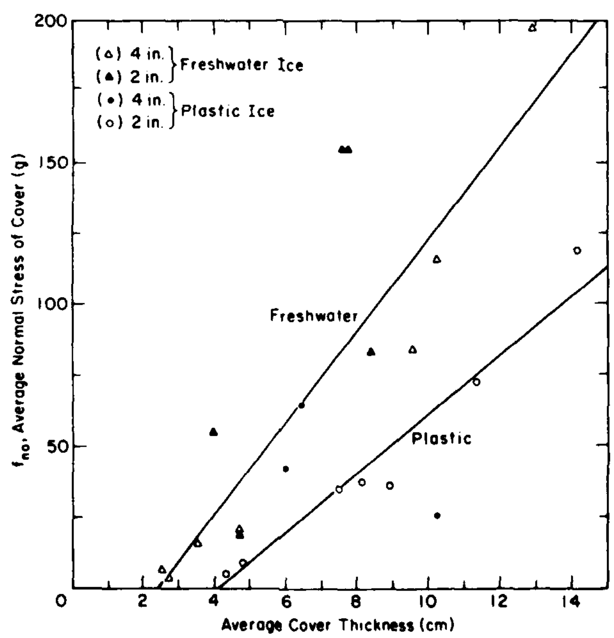

Figure 6. Average normal force produced by restraining the ice cover and stopping it from spreading laterally.

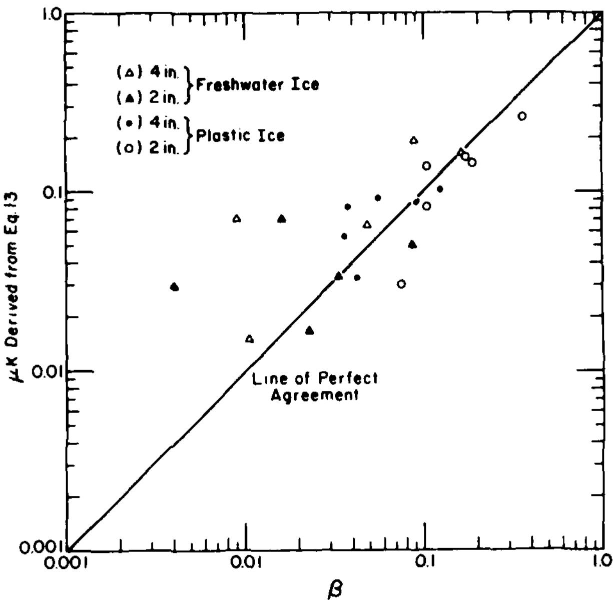

Figure 7. Comparison of the value of μK derived from eq 13 and the value of β derived from eq 7.

against a restraining boom. Local differences in cover thickness, undercover shear stress application, etc., will greatly influence the normal forces experienced by the shorelines.

Data scatter

The equations developed to describe the force distribution in a fragmented ice cover assumed a uniform material with isotropic properties. However, this set of conditions was not completely realized in these experiments. The rectangular blocks that constituted the ice cover were uniform in size. However, the average size of a model ice fragment was large when compared to the average thickness of the cover. The cover could only be considered to be approaching "granular."

Fragmented ice covers observed in the field are seldom granular in appearance. Often, when the fragmented ice covers were formed upstream of the restraining boom, the floating ice fragments deposited themselves in the cover in a very uniform, regular manner. The fragmented cover was manually thickened and stirred to make the model ice blocks' orientation more random and to approach isotropic conditions. However, idealized granularity and isotropic material properties were not achieved and this probably contributed to the data scatter.

The ice covers were not completely uniform in thickness, and the relationship of the cover thickness to the measured normal force has been shown. The shear stress of the flowing water undoubtedly was not uniformly applied to the bottom of the fragmented cover. Therefore, the averaging procedures used in the analysis would introduce some errors and also contribute to the data scatter.

Melting of the freshwater ice covers also undoubtedly contributed to the data scatter. Melting was continuous during the course of a test, and although each test series was conducted as quickly as possible, it was probably a factor.

SUMMARY AND CONCLUSIONS

This investigation showed that the forces associated with a fragmented ice cover could be measured in a laboratory flume. The measurement apparatus worked well, though the results are dependent on the type of material used to model the fragmented cover. The coefficient of friction differed by an order of magnitude between the polyethylene and freshwater ice blocks. Force measurement panels with greater absolute roughness may tend to minimize this difference; however, increased water shear on the force measurement panels, because of this greater roughness, would tend to complicate the measurement procedures.

The measured boom force followed a pattern of asymptotically approaching a maximum as the cover length was increased, as predicted by earlier investigators. However, unless corrections were made to account for the forces caused by keeping the fragmented cover from spreading, the coefficients of the equation describing the boom force did not equal those measured.

The boom force could be adequately predicted using the values of coefficients averaged over the entire cover upstream of the boom. The forces experienced by the shoreline, however, were influenced greatly by the local conditions of the cover and were therefore difficult to predict.

The data scatter was large, especially for the freshwater ice. The theories developed to describe the forces in a fragmented cover assume a uniform granular material. However, the fragmented covers investigated were made of rectangular blocks whose dimensions were significant when compared to the thickness of the cover. The fragmented covers also had local differences in thickness and packing densities. For these reasons the data were quite scattered.

LITERATURE CITED

Berdennikov, V.P. (1964) Dynamic conditions of formation of ice jams on rivers. *Soviet Hydrology*, Selected Papers, no. 2.

Cowin, S.C. (1977) The theory of static loads in bins. *American Society of Mechanical Engineers Journal of Applied Mechanics*, **44**: 409-412.

Janssen, H.A. (1895) Versuche uber Getreidedruck in Silozellen. *Zeitschrift Verein Deutscher Ingenieure*, **39**: 1045-1049.

Mellor, M. (1979) Towing ships through ice-clogged channels by warping and kedging. USA Cold Regions Research and Engineering Laboratory, CRREL Report 79-21. ADA077801.

Michel, B. (1978) *Ice Mechanics*. Quebec, Canada: Les Presses de l'Université Laval.

Pariset, E. and R. Hausser (1961) Formation and evaluation of ice covers on rivers. *Transactions of the Engineering Institute of Canada*, **5**: 41-49.

Pariset, E., R. Hausser and A. Gagnon (1966) Formation of ice covers and ice jams in rivers. *American Society of Civil Engineers Journal of the Hydraulics Division*, **HY6**: 1-23.

Sodhi, D.S. and W.F. Weeks (1978) Ice arching and the drift of pack ice through channels. In *International Association of Hydraulic Research, Proceedings, Symposium on Ice Problems, August 7-9, Lulea, Sweden*, p. 415-432.

Tatinclaux, J.C., C.L. Lee, T.P. Wang, T. Nakato and J.F. Kennedy (1977) A laboratory investigation of the mechanics and hydraulics of river ice jams. USA Cold Regions Research and Engineering Laboratory, CRREL Report 77-9. ADA032471.

the equation describing the boom force did not equal those measured.

The boom force could be adequately predicted using the values of coefficients averaged over the entire cover upstream of the boom. The forces experienced by the shoreline, however, were influenced greatly by the local conditions of the cover and were therefore difficult to predict.

The data scatter was large, especially for the freshwater ice. The theories developed to describe the forces in a fragmented cover assume a uniform granular material. However, the fragmented covers investigated were made of rectangular blocks whose dimensions were significant when compared to the thickness of the cover. The fragmented covers also had local differences in thickness and packing densities. For these reasons the data were quite scattered.

LITERATURE CITED

Berdennikov, V.P. (1964) Dynamic conditions of formation of ice jams on rivers. *Soviet Hydrology*, Selected Papers, no. 2.

Cowin, S.C. (1977) The theory of static loads in bins. *American Society of Mechanical Engineers Journal of Applied Mechanics*, **44**: 409–412.

Janssen, H.A. (1895) Versuche uber Getreidedruck in Silozellen. *Zeitschrift Verein Deutscher Ingenieure*, **39**: 1045–1049.

Mellor, M. (1979) Towing ships through ice-clogged channels by warping and kedging. USA Cold Regions Research and Engineering Laboratory, CRREL Report 79-21. ADA077801.

Michel, B. (1978) *Ice Mechanics*. Quebec, Canada: Les Presses de l'Université Laval.

Pariset, E. and R. Hausser (1961) Formation and evaluation of ice covers on rivers. *Transactions of the Engineering Institute of Canada*, 5: 41–49.

Pariset, E., R. Hausser and A. Gagnon (1966) Formation of ice covers and ice jams in rivers. *American Society of Civil Engineers Journal of the Hydraulics Division*, **HY6**: 1-23.

Sodhi, D.S. and W.F. Weeks (1978) Ice arching and the drift of pack ice through channels. In *International Association of Hydraulic Research, Proceedings, Symposium on Ice Problems, August 7-9, Lulea, Sweden*, p. 415–432.

Tatinclaux, J.C., C.L. Lee, T.P. Wang, T. Nakato and J.F. Kennedy (1977) A laboratory investigation of the mechanics and hydraulics of river ice jams. USA Cold Regions Research and Engineering Laboratory, CRREL Report 77-9. ADA032471.

APPENDIX A: EXPERIMENTAL RESULTS

Avg. shear (Pa)	Boom force (g)	Cover length (m)	Ice cover forces (g) Section 1 Shear	Section 1 Normal	Section 2 Shear	Section 2 Normal	Section 3 Shear	Section 3 Normal	Section 4 Shear	Section 4 Normal	Section 5 Shear	Section 5 Normal
				Experiment 42								
1.021	65.88	0.914	9.59	47.45								
1.059	154.69	1.828	9.34	42.22	1.55	49.01						
2.187	325.53	2.742	31.93	93.71	45.85	124.72	32.80	108.28				
2.004	355.11	3.656	31.66	103.23	53.62	150.18	39.28	112.52	31.90	80.76		
1.796	365.09	4.570	32.35	107.45	58.53	163.61	42.61	115.46	38.77	102.55	19.26	29.95
0.000	396.08	7.315	41.30	123.16	54.68	163.52	40.79	132.64	45.40	118.36	58.86	66.08
				Experiment 43								
2.346	164.04	0.914	15.72	78.28								
1.765	274.98	1.828	3.64	110.91	5.99	39.04						
1.691	277.46	2.742	17.71	124.85	17.60	58.42	37.35	80.26				
1.450	291.20	3.656	27.69	134.45	25.57	98.37	31.49	113.72	11.29	39.06		
1.442	348.96	4.570	29.64	147.31	28.18	108.11	37.31	111.00	19.52	52.63	11.30	49.19
0.000	382.36	7.315	25.01	142.66	28.94	105.93	39.41	96.79	35.39	70.46	19.11	58.15
				Experiment 44								
6.347	522.64	0.914	3.12	25.98								
3.987	634.91	1.828	8.22	49.87	6.60	27.82						
3.636	721.60	2.742	29.48	102.44	29.86	75.72	34.31	86.61				
3.211	777.47	3.656	39.55	131.85	42.05	109.30	50.47	131.10	14.29	33.48		
2.879	789.32	4.570	44.60	138.81	48.76	132.13	48.78	123.40	34.50	63.03	28.48	48.28
0.000	793.56	7.315	40.74	130.25	61.61	176.21	50.33	138.51	79.07	111.59	105.51	146.71
				Experiment 46								
0.429	19.21	0.914	8.26	20.70								
0.519	43.48	1.828	11.76	21.71	9.78	32.10						
0.577	46.24	2.742	23.75	23.56	8.09	35.96	17.17	57.68				
0.609	56.66	3.656	22.79	26.34	16.00	54.12	22.74	51.95	11.67	59.72		
0.549	64.47	4.570	21.87	22.93	17.73	56.69	20.27	60.94	6.95	60.82	15.31	58.18
0.000	66.31	7.315	21.27	23.75	17.85	56.71	16.30	62.34	14.33	63.25	12.19	68.17
				Experiment 48								
1.073	85.44	0.914	1.99	41.48								
1.212	149.76	1.828	6.43	46.46	19.70	57.08						
1.823	233.85	2.742	23.72	78.38	44.24	105.39	43.00	66.74				
1.510	250.54	3.656	26.67	90.83	49.80	120.97	46.46	76.44	3.58	35.61		
2.181	330.54	4.570	45.73	137.88	56.08	135.08	79.73	139.13	24.19	62.23	83.31	164.49
0.000	366.67	7.315	47.75	155.99	68.67	167.58	86.77	149.57	52.19	102.90	117.95	229.62
				Experiment 49								
4.062	264.82	0.919	36.81	77.13								
5.005	529.53	1.828	84.39	111.10	67.93	76.34						
3.863	588.59	2.742	93.71	135.33	76.14	107.47	11.65	40.19				
3.505	652.82	3.656	95.17	155.20	82.15	115.82	44.33	85.10	36.08	65.47		
3.024	672.66	4.570	106.67	171.70	74.75	118.17	50.92	97.55	37.96	72.45	23.41	76.86
0.000	758.36	7.315	122.47	187.37	84.62	145.11	82.38	167.53	110.25	172.74	72.24	137.94

APPENDIX A: EXPERIMENTAL RESULTS

Avg. shear (Pa)	Boom force (g)	Cover length (m)	Ice cover forces (g) Section 1 Shear	Section 1 Normal	Section 2 Shear	Section 2 Normal	Section 3 Shear	Section 3 Normal	Section 4 Shear	Section 4 Normal	Section 5 Shear	Section 5 Normal
					Experiment 42							
1.021	65.88	0.914	9.59	47.45								
1.059	154.69	1.828	9.34	42.22	1.55	49.01						
2.187	325.53	2.742	31.93	93.71	45.85	124.72	32.80	108.28				
2.004	355.11	3.656	31.66	103.23	53.62	150.18	39.28	112.52	31.90	80.76		
1.796	365.09	4.570	32.35	107.45	58.53	163.61	42.61	115.46	38.77	102.55	19.26	29.95
0.000	396.08	7.315	41.30	123.16	54.68	163.52	40.79	132.64	45.40	118.36	58.86	66.08
					Experiment 43							
2.346	164.04	0.914	15.72	78.28								
1.765	274.98	1.828	3.64	110.91	5.99	39.04						
1.691	277.46	2.742	17.71	124.85	17.60	58.42	37.35	80.26				
1.450	291.20	3.656	27.69	134.45	25.57	98.37	31.49	113.72	11.29	39.06		
1.442	348.96	4.570	29.64	147.31	28.18	108.11	37.31	111.00	19.52	52.63	11.30	49.19
0.000	382.36	7.315	25.01	142.66	28.94	105.93	39.41	96.79	35.39	70.46	19.11	58.15
					Experiment 44							
6.347	522.64	0.914	3.12	25.98								
3.987	634.91	1.828	8.22	49.87	6.60	27.82						
3.636	721.60	2.742	29.48	102.44	29.86	75.72	34.31	86.61				
3.211	777.47	3.656	39.55	131.85	42.05	109.30	50.47	131.10	14.29	33.48		
2.879	789.32	4.570	44.60	138.81	48.76	132.13	48.78	123.40	34.50	63.03	28.48	48.28
0.000	793.56	7.315	40.74	130.25	61.61	176.21	50.33	138.51	79.07	111.59	105.51	146.71
					Experiment 46							
0.429	19.21	0.914	8.26	20.70								
0.519	43.48	1.828	11.76	21.71	9.78	32.10						
0.577	46.24	2.742	23.75	23.56	8.09	35.96	17.17	57.68				
0.609	56.66	3.656	22.79	26.34	16.00	54.12	22.74	51.95	11.67	59.72		
0.549	64.47	4.570	21.87	22.93	17.73	56.69	20.27	60.94	6.95	60.82	15.31	58.18
0.000	66.31	7.315	21.27	23.75	17.85	56.71	16.30	62.34	14.33	63.25	12.19	68.17
					Experiment 48							
1.073	85.44	0.914	1.99	41.48								
1.212	149.76	1.828	6.43	46.46	19.70	57.08						
1.823	233.85	2.742	23.72	78.38	44.24	105.39	43.00	66.74				
1.510	250.54	3.656	26.67	90.83	49.80	120.97	46.46	76.44	3.58	35.61		
2.181	330.54	4.570	45.73	137.88	56.08	135.08	79.73	139.13	24.19	62.23	83.31	164.49
0.000	366.67	7.315	47.75	155.99	68.67	167.58	86.77	149.57	52.19	102.90	117.95	229.62
					Experiment 49							
4.062	264.82	0.919	36.81	77.13								
5.005	529.53	1.828	84.39	111.10	67.93	76.34						
3.863	588.59	2.742	93.71	135.33	76.14	107.47	11.65	40.19				
3.505	652.82	3.656	95.17	155.20	82.15	115.82	44.33	85.10	36.08	65.47		
3.024	672.66	4.570	106.67	171.70	74.75	118.17	50.92	97.55	37.96	72.45	23.41	76.86
0.000	758.36	7.315	122.47	187.37	84.62	145.11	82.38	167.53	110.25	172.74	72.24	137.94

Avg. shear (Pa)	Boom force (g)	Cover length (m)	Ice cover forces (g) Section 1 Shear	Section 1 Normal	Section 2 Shear	Section 2 Normal	Section 3 Shear	Section 3 Normal	Section 4 Shear	Section 4 Normal	Section 5 Shear	Section 5 Normal
					Experiment 50							
2.719	217.68	0.914	4.44	25.47								
1.710	261.44	1.828	7.96	34.65	3.78	30.46						
1.509	307.93	2.742	13.17	46.18	5.69	34.44	15.73	22.71				
1.572	387.45	3.656	20.13	54.65	18.71	58.92	22.79	46.95	6.67	70.12		
1.493	418.08	4.570	23.09	66.01	16.45	57.19	37.42	46.37	10.01	45.65	15.01	13.43
0.000	487.62	6.40	28.17	79.89	30.89	95.02	66.32	99.83	41.21	107.34	53.61	111.41
					Experiment 54							
0.225	26.77	0.914	-4.00	16.63								
0.411	32.21	1.828	9.84	44.39	8.31	39.98						
0.694	59.09	2.742	17.71	59.54	14.49	54.11	24.98	41.70				
0.663	71.59	3.656	20.79	70.67	17.55	58.93	30.52	56.12	5.79	41.22		
0.686	96.64	4.570	24.49	83.53	18.51	64.95	32.71	69.04	10.93	51.06	7.85	70.24
0.000	131.55	8.23	42.29	110.86	31.07	87.10	72.43	145.06	119.04	180.10	194.10	279.75
					Experiment 55							
1.269	128.59	0.914	-11.41	132.06								
2.140	215.94	1.828	41.98	179.87	28.34	161.55						
5.155	431.81	2.742	164.85	344.30	171.23	386.34	92.41	362.58				
4.880	474.31	3.656	212.92	372.08	207.33	449.75	113.13	475.81	42.71	157.85		
4.372	479.78	4.570	209.44	371.31	206.45	466.95	113.92	491.92	83.34	226.58	57.80	126.72
0.000	560.00	5.486	223.16	400.11	216.97	505.03	143.05	542.42	126.10	304.47	143.41	294.97
					Experiment 56							
1.495	107.01	0.914	8.78	79.77								
1.106	152.40	1.828	11.17	101.50	4.75	77.77						
1.038	182.45	2.742	17.28	118.42	11.27	97.26	10.00	84.89				
1.262	197.98	3.656	28.98	136.09	26.22	118.49	44.18	124.89	11.93	73.31		
1.347	209.39	4.570	38.60	134.38	26.97	122.55	49.92	132.67	29.48	91.65	30.93	100.95
0.000	222.40	7.315	44.35	138.16	32.01	132.33	61.28	150.38	68.11	127.96	74.99	179.30
					Experiment 57							
0.214	12.29	0.914	2.78	9.42								
0.221	21.95	1.828	4.91	20.67	2.50	9.68						
0.281	31.80	2.742	8.98	28.42	6.08	17.77	4.15	18.69				
0.322	42.27	3.656	12.33	34.84	8.69	25.45	6.61	18.78	4.96	16.05		
0.318	53.44	4.570	13.97	40.33	7.38	27.31	7.66	21.09	5.30	20.44	5.18	12.87
0.000	73.86	9.144	13.13	42.79	9.16	30.85	16.65	27.79	16.72	35.88	15.60	32.56
					Experiment 58							
0.953	65.46	0.914	6.98	47.75								
0.727	94.92	1.828	8.25	49.22	4.88	35.96						
0.658	116.46	2.742	9.57	55.59	5.26	48.00	9.25	46.88				
0.619	123.12	3.656	11.72	59.04	9.74	52.58	16.06	53.10	4.09	42.75		
0.506	130.29	4.570	10.98	60.13	9.52	52.46	16.71	57.11	5.05	46.31	-1.93	39.92
0.000	132.81	6.401	11.88	60.10	12.26	53.24	21.01	61.11	13.79	55.36	31.79	59.58
					Experiment 59							
0.295	11.77	0.914	6.42	3.74								
0.202	20.69	1.828	5.32	7.27	1.14	5.81						
0.253	35.77	2.742	7.82	15.11	4.58	13.15	1.34	9.70				
0.245	37.59	3.656	9.84	16.60	1.31	15.28	2.85	12.07	7.98	7.15		
0.218	38.31	4.570	9.83	18.04	1.31	16.31	6.27	16.00	8.47	12.44	0.35	8.04
0.000	38.53	9.144	10.41	18.53	2.20	16.76	7.54	18.60	11.66	17.16	11.75	15.45

Avg. shear (Pa)	Boom force (g)	Cover length (m)	Ice cover forces (g) Section 1 Shear	Section 1 Normal	Section 2 Shear	Section 2 Normal	Section 3 Shear	Section 3 Normal	Section 4 Shear	Section 4 Normal	Section 5 Shear	Section 5 Normal
					Experiment 60							
0.585	43.60	0.914	2.58	36.76								
0.380	53.57	1.828	-1.62	42.20	6.53	44.13						
0.439	63.12	2.742	5.76	52.95	10.78	48.26	6.84	34.30				
0.400	64.64	3.656	7.30	55.61	12.25	48.27	5.73	36.53	9.13	41.01		
0.422	67.16	4.570	9.01	54.99	12.35	47.38	9.06	38.43	8.29	38.73	15.65	42.25
0.000	77.38	9.144	8.70	54.91	11.39	48.32	11.48	41.98	14.09	42.66	19.62	49.19
					Experiment 63							
0.305	21.39	0.914	2.02	4.06								
0.242	34.07	1.828	1.92	7.40	1.23	2.85						
0.185	39.35	2.742	1.58	9.26	1.17	4.47	0.73	3.86				
0.184	33.41	3.656	8.98	12.01	2.63	5.13	0.42	4.80	2.00	9.27		
0.173	25.93	4.570	14.19	13.58	3.72	7.24	0.27	7.18	3.56	12.12	1.33	1.33
0.000	49.11	5.486	8.57	17.03	3.49	7.43	0.42	7.18	5.44	13.14	0.79	5.30
					Experiment 64							
0.204	18.21	0.914	-0.61	2.10								
0.165	24.49	1.828	0.75	3.97	0.76	-0.64						
0.157	25.40	2.742	0.53	4.28	0.66	-0.68	3.21	26.66				
0.131	28.51	3.656	6.04	9.18	0.63	0.09	0.85	17.51	0.12	1.15		
0.116	42.35	4.570	2.36	5.36	0.53	1.92	0.18	8.19	0.10	1.92	-0.16	2.24
0.000	46.77	5.486	0.12	7.10	0.47	3.05	0.13	5.29	2.17	3.68	0.56	3.33
					Experiment 65							
.388	29.32	0.919	1.53	3.43								
[illegible]	35.02	1.828	4.04	2.31	1.36	6.75						
.326	42.85	2.742	7.24	0.89	1.58	5.92	10.51	4.24				
.309	50.12	3.656	11.21	5.29	0.69	7.45	7.34	2.14	7.22	29.81		
.289	56.98	4.570	19.52	8.25	0.84	7.13	3.95	9.99	4.36	26.56	3.02	44.28
[illegible]	62.08	5.486	24.63	12.72	1.00	5.44	4.16	15.02	5.09	34.58	3.92	57.31
					Experiment 66							
.696	45.64	0.914	6.20	7.68								
0.481	56.86	1.828	6.14	18.79	5.48	6.28						
0.529	100.37	2.742	7.03	38.75	4.74	28.95	4.12	30.55				
0.517	124.84	3.656	6.54	29.11	4.02	29.09	3.99	50.71	9.13	24.37		
0.466	154.99	4.570	6.69	40.63	4.95	29.52	4.59	54.28	2.71	20.73	0.71	29.71
0.000	225.99	5.486	6.86	41.37	4.59	29.56	3.30	68.33	5.02	20.66	2.16	35.05
					Experiment 67							
1.458	115.45	0.914	3.00	54.02								
1.046	161.68	1.828	4.34	63.50	2.02	71.06						
0.862	207.40	2.792	4.73	91.35	2.84	62.70	-3.51	131.19				
0.964	303.43	3.656	4.93	110.36	4.06	70.21	-6.69	164.35	6.59	45.01		
1.217	473.01	4.570	10.02	115.75	1.20	85.98	-6.33	179.75	12.16	93.65	-0.03	118.56
0.000	534.36	5.486	18.49	150.55	0.74	98.65	-2.47	190.67	11.69	108.90	7.72	161.59
					Experiment 68							
2.211	168.46	0.914	7.88	40.29								
1.800	288.53	1.828	3.91	55.83	1.80	143.34						
2.144	486.12	2.742	4.37	88.78	2.07	107.38	18.53	121.37				
3.343	754.83	3.656	6.10	100.59	1.65	102.53	8.54	162.88	163.36	111.29		
2.521	845.43	4.570	5.17	105.85	1.03	95.31	1.67	153.38	93.22	165.86	1.45	110.99
0.000	762.63	6.401	7.16	113.59	-3.36	132.34	7.75	165.41	175.79	147.53	11.09	147.82

Avg. shear (Pa)	Boom force (g)	Cover length (m)	Ice cover forces (g) Section 1 Shear	Normal	Section 2 Shear	Normal	Section 3 Shear	Normal	Section 4 Shear	Normal	Section 5 Shear	Normal
					Experiment 69							
11.878	981.00	0.914	4.37	221.78								
8.304	1377.65	1.828	1.99	241.67	1.13	91.28						
6.999	1721.30	2.742	2.28	276.91	3.37	149.98	8.52	280.91				
6.489	2114.70	3.656	2.82	286.97	0.44	194.17	14.09	500.73	6.66	234.00		
6.170	2464.53	4.570	0.48	301.57	8.24	211.29	33.39	496.95	24.12	193.59	-13.13	107.74
9.855	2901.85	6.401	407.47	667.62	-9.15	512.29	169.64	648.10	17.70	220.83	16.40	203.78
					Experiment 70							
1.306	104.30	0.914	2.25	13.37								
0.340	47.56	1.828	3.75	8.69	0.78	7.27						
0.238	49.19	2.742	3.98	26.08	0.67	15.15	0.50	24.42				
0.214	55.69	3.656	6.79	21.34	0.71	15.69	0.24	19.08	0.16	21.29		
0.190	66.24	4.570	6.77	23.89	0.62	17.74	-0.15	39.11	0.19	16.14	-0.95	31.02
0.000	63.29	8.230	6.40	20.48	0.70	15.54	0.91	33.90	0.45	12.52	-0.08	23.41
					Experiment 72							
0.457	31.68	0.910	3.19	34.95								
0.390	59.46	0.828	2.25	8.93	0.49	19.20						
0.859	185.04	2.742	5.41	33.25	2.85	44.42	6.56	124.48				
0.903	241.62	3.656	12.42	34.19	1.33	41.30	3.08	101.09	12.78	76.42		
0.808	305.25	4.570	4.41	51.79	2.01	52.30	2.72	116.87	4.34	61.56	2.19	38.53
0.000	357.28	5.486	11.96	65.66	3.48	72.36	1.59	126.60	4.05	63.30	5.13	47.46
					Experiment 73							
6.572	537.14	0.914	5.26	184.87								
1.756	278.24	1.828	4.50	164.54	2.69	132.52						
1.154	272.41	2.742	2.08	156.85	1.80	126.21	4.22	253.78				
0.949	294.76	3.656	5.53	197.02	2.51	130.89	5.15	226.23	-2.46	140.82		
1.004	392.81	4.570	8.58	198.29	3.21	128.43	5.90	220.89	-1.05	124.94	-3.92	115.41
0.000	455.98	7.315	11.29	185.13	2.64	119.84	2.68	214.84	-1.17	112.28	2.89	89.73
					Experiment 74							
2.549	196.87	0.914	7.78	134.78								
3.099	473.72	1.828	11.76	177.84	9.60	174.04						
3.116	678.05	2.742	21.75	224.45	9.12	195.32	19.57	113.68				
2.620	769.59	3.656	24.83	255.09	9.85	212.41	18.72	125.78	-1.55	63.76		
2.744	986.14	4.570	53.70	276.10	9.56	228.41	11.83	140.87	-0.30	69.55	3.85	89.36
0.000	1067.09	5.416	76.72	281.40	10.36	245.36	10.16	158.14	0.03	75.21	3.67	133.01
					Experiment 75							
3.064	222.14	0.914	16.59	401.32								
2.434	346.35	1.828	16.04	346.32	13.60	142.67						
2.023	386.26	2.742	16.94	347.73	15.91	153.70	26.91	79.64				
1.735	419.46	3.656	14.98	311.41	24.56	151.87	25.47	67.48	14.46	197.31		
1.444	467.59	9.570	16.72	291.24	28.52	143.06	14.57	69.50	7.60	172.09	-0.37	233.66
0.000	569.19	5.791	26.12	282.18	32.34	149.47	5.53	120.99	5.69	181.00	6.47	262.31

A facsimile catalog card in Library of Congress MARC format is reproduced below.

Stewart, Douglas
Force distribution in a fragmented ice cover / by Douglas Stewart and Steven F. Daly. Hanover, N.H.: Cold Regions Research and Engineering Laboratory; Springfield, Va.: available from National Technical Information Service, 1984.
iv, 22 p., illus.; 28 cm. (CRREL Report 84-7.)
Bibliography: p. 11.
1. Flume tests. 2. Ice. 3. Ice booms. 4. Ice forces. 5. Laboratory tests. 6. River ice.
I. Daly, Steven F. II. United States. Army. Corps of Engineers. III. Cold Regions Research and Engineering Laboratory, Hanover, N.H. IV. Series: CRREL Report 84-7.

DAT

FILM

7 —